Lasers in Manufacturing Conference 2023

Effect of femtosecond pulsed laser micromachining parameters on acoustic emission process monitoring signals

Kerim Yildirim[a,*], Joselito Yam Alcaraz II[b], Balasubramanian Nagarajan[a], Tegoeh Tjahjowidodo[b], Sylvie Castagne[a]

[a]*KU Leuven, Department of Mechanical Engineering and Flanders Make@KU Leuven-M&A, B-3001 Leuven, Belgium*
[b]*KU Leuven, Department of Mechanical Engineering, B-2860 Sint-Katelijne-Waver, Belgium*

Abstract

Micromachining with a ultrashort pulse (USP) laser is a widely-employed manufacturing process for numerous applications such as biomedical devices, micro-components and electronics. During USP ablation, shock waves are associated with the ablation mechanism. Acoustic emission (AE) monitoring is a non-destructive approach for monitoring shock wave behavior during laser micromachining. The produced AE signals are significantly influenced by USP laser parameters such as pulse energy, pulse repetition rate and number of pulses. Using time- and frequency-based analysis techniques, the correlation between these laser characteristics and the AE signals generated by the femtosecond laser pulses are investigated. The results indicate that AE signal intensity increases as pulse energy and number of pulses increase, indicating a greater degree of material removal. These findings can be utilized to optimize AE-based monitoring methodology for laser micromachining conditions for specific materials and applications.

Keywords: Ultra-short pulsed laser; femtosecond laser micromachining; real-time monitoring; acoustic emission sensing

1. Introduction

Ultra-short pulsed (USP) lasers, particularly femtosecond (fs) lasers, have become a popular tool for manufacturing micro-structures due to their versatility and ability to achieve high-precision and high-quality material micro-processing (Mazur et al., 2015). Almost any material can be shaped with minimal or no thermal

* Corresponding author.

damage using fs lasers (Ostendorf et al., 2006). Compared to conventional nanosecond (ns) laser machining (Fig. 1a.), fs laser pulses induce exceptionally high peak power densities with low pulse energies, resulting in a limited heat-affected zone (Hamad, 2016), precise micro processing (Orazi et al., 2021), and reduced mechanical and thermal damage (Le Harzic et al. 2005). The non-thermal characteristics of fs ablation are required for many applications to ensure that the material properties are maintained even near the processing zone (Ion et al., 2005). Current needs in high-technology industries, such as semiconductor, optics, MEMS, etc., have necessitated such development of manufacturing techniques that can reliably produce ever-smaller features with extremely tight tolerances (Lee et al., 2006). Femtosecond laser pulses have numerous benefits including efficient, rapid, and localized energy deposition, well-defined ablation thresholds, negligible thermal and structural damage.

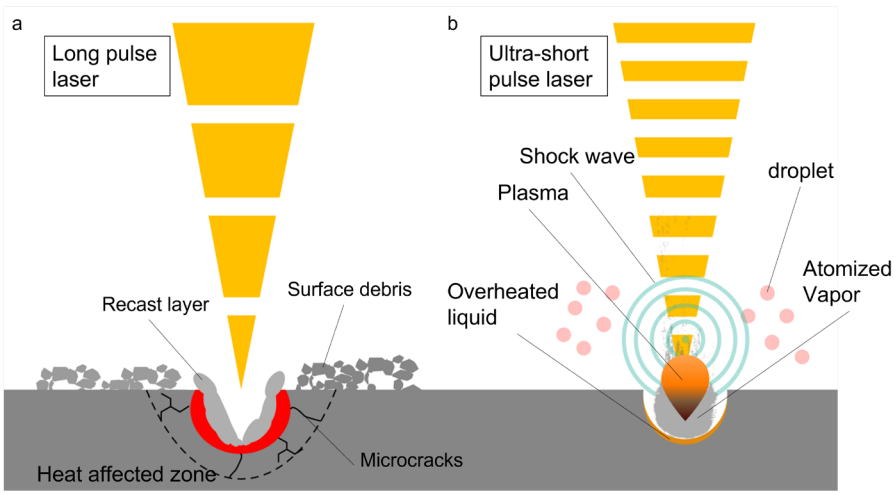

Fig. 1. Schematical illustration of (a) nanosecond pulse laser; (b) femtosecond pulsed laser

However, fs laser micromachining is a complex process due to complex interactions between materials, process settings, and energy sources, while the underlying material-removal mechanisms are not well understood (Mozaffar et al., 2022). In addition, tight component tolerances and long cycle times present new obstacles for laser micromachining. As laser processes are influenced by a variety of factors related to machine, workpiece, and processing condition related factors, even slight parameter changes might result in components falling outside of the required tolerances. Therefore, the range of acceptable parameter deviations, also known as the process window, is exceedingly narrow for the fabrication of precision components (Lee et al., 2006).

To achieve the desired geometry of the processed structure, the optimal processing parameters (e.g., wavelength, pulse energy, pulse duration, pulse repetition rate, beam spot size, focal point, and scanning speed) for the target material should first be identified (Wiesemann, 2004). The process parameter optimization in fs laser processing is typically performed experimentally due to the complexity of the underlying process mechanisms and the corresponding lack of physics-based models (Linde et al., 2000). Due to the multiscale and multi-physics nature of fs laser processing and its complex boundary conditions, it has been difficult to develop physics-based modeling to comprehend the mechanisms that occur during fs laser processing. In addition, it requires expensive computational resources and significant simulation time (Francois et al., 2017). Physics-based modeling and trial-and-error experiments are usually time-consuming

and expensive due to the large number of process and material parameters (Rußbüldt et al., 2010). Moreover, traditional post-characterization techniques, such as X-ray computed tomography (CT), atomic force microscopy (AFM) and scanning electron microscopy (SEM) are time- and cost-intensive, and their implementations are constrained by production scale (Schmitt et al., 2014).

To address these limitations related to process modeling and offline characterization in the context of fs laser processing, an in-situ process monitoring approach has been proposed (Terchi & Au, 2001) (Li & Guan, 2020). Sensor-based monitoring provides useful information about the manufacturing process that can serve the dual function of process control and quality monitoring (Lee et al., 2006). Current sensing techniques in fs laser process monitoring include monitoring with optical- (Roozbahani et. al., 2017), thermal- (Bornschlegel et. al., 2020) or AE-based sensors (Xie, Zhang, et al., 2021). The collection of reliable data depends upon the monitoring systems. Nemeth et al. used optical coherence tomography to monitor the fs laser processing of surface textures (Nemeth et al., 2013). However, the limitations of optical techniques remains since there is a trade-off between imaging speed and resolution. While OCT provides high-resolution imaging, the acquisition speed is slow, limiting its real-time monitoring capabilities (Liu et. al. 2018). The integration of imaging systems and photodiodes (Singha et. al., 2008) enabled the real-time monitoring of laser-generated plasma plume and ablation dynamics. However, a limitation arises when attempting to detect and monitor weak or transient signals. This challenge is attributed to factors such as noise, limited dynamic range, and constrained temporal resolution, which hinders the detection of rapid changes in signal intensity.

Alternatively, AE-based technique is being widely used in laser-based manufacturing for processes such as laser welding (Lu et al., 2021), laser cutting (Kek et al., 2009) and laser derusting (Xie, Huang, et al., 2022) to monitor the processing quality. AE refers to the short elastic wave produced by the sudden release of strain energy due to deformation or damage inside or on the surface of the materials (Chethan et al., 2019)(Bhuiyan et al., 2016). In their earlier work, Bordatchev et al. studied the impact of the focal position during ns-laser pulsed processing using AE sensors and found that statistical properties of the measured AE signal correlated with the focus position (Bordatchev et al., 2006). Recently, Kacaras et al. investigated the same for picosecond laser processing, showing the correlation between focal position solid-borne emission sensor (SBAE) sensor signals using time-frequency analysis (Kacaras et al., 2019).

X. Xie et al. investigated the specific spectrum of various derusting settings and differentiated RMS signal characteristics. They have found that the changes in rust removal conditions and the effect of derusting parameters can be precisely mapped by monitoring AE signals in the time and frequency domain. The same group of researchers demonstrates the association between material removal, surface structure characteristics, surface defects, and acoustic emission signals in metal derusting (Xie, Zhang, et al., 2021) and fs laser ablation of Si (Xie, Huang, et al., 2022). R. Yang used AE sensor to evaluate the quality of ns laser cutting on composite materials by AE signals of laser-induced plasma in frequency domain and wavelet analysis, which provided a new solution for observing and studying laser-induced plasma (Yang et al., 2022).

Despite the initial efforts on AE-based process monitoring of fs laser ablation in the literature, there are limited studies on understanding the process evolution at a finer process timescale (one to several pulses) using AE sensors. Moreover, the experiments described in the literature were conducted using low-speed sampling rates and sensors with restricted frequency bands, which may not provide adequate resolution for ultra-short pulse lasers, particularly femtosecond lasers. In this paper, we aim to analyze the effect of laser parameters on the acoustic emission signal during laser processing with single- and multi-pulses. To analyze the effect of fs laser pulses on AE signal characteristics, single parameter analysis, correlation analysis, and continuous wavelet transform (CWT) method are employed. The relationship between material removal with pulses, and natural behavior of acoustic emission signals is studied.

2. Experimental setup

The methodology employed to investigate the correlation between the AE signals during fs laser ablation and the corresponding feature dimensions is described in this section. The optical-mechanical system used for fs laser micromachining comprises a fs laser source, optical beam delivery components, a 5-axes mechanical air bearing stages and 2-axes optical galvo-scanner, and electronic control units. The technical features of the fs laser system (Carbide, Light Conversion) used for the experiments including pulse duration, wavelength, repetition rate, and maximum average power along with galvanometric scanner and f-theta lens are presented in Table 1.

Table 1. Laser system characteristics and ablation parameters used for experiments

Characteristics	Units	Values
Wavelength	nm	1030
Pulse duration	fs	250
Repetition rate	kHz	200
Max. average power	W	20
Focused spot diameter	µm	20
Pulse energy	µJ	10 to 100
Focal distance	mm	118
Max Optical scanning speed	mm/s	3000
Max mechanical stage speed	mm/s	300

The experiments were aimed at understanding the correlation between the AE signals during the fs laser ablation and the corresponding ablation regime. To achieve this, a monitoring system was integrated into the laser micromachining system. The monitoring system which consists of a SBAE sensor, a preamplifier, a data acquisition system, and signal processing evaluation system is used to detect the high-frequency signals generated during the ablation process. The laser-induced shock waves propagated through the sample were detected by AE sensors that were mounted on the steel plate (316L with the size of 25x90 mm^2)at a distance of 10 mm from the ablation zone (Fig. 2.). For the detection of the acoustic emissions, a wideband AE sensor (AE1045S, Vallen Systems) was used. It is a structure-borne piezoelectric detector for acoustic emission of shock waves with a frequency ranging from 100 kHz to 1500 kHz. The sensor detects the high-frequency energy signals to be measured and delivers an electrical signal proportional to the quantity detected as an output signal. The signal was then fed through a preamplifier (AEP5) with different frequency bandwidths. The preamplifier is set to the gain of 40 dB in order to collect the AE signal and distinguish it from the environment noise. The preamplifiers in combination with a decoupling box provide signal amplification and impedance matching to the input of the data acquisition system (DAQ) at a sampling rate of 14 MHz. The computer connected to the data acquisition system with the LabVIEW software from NI serves as the measurement system.

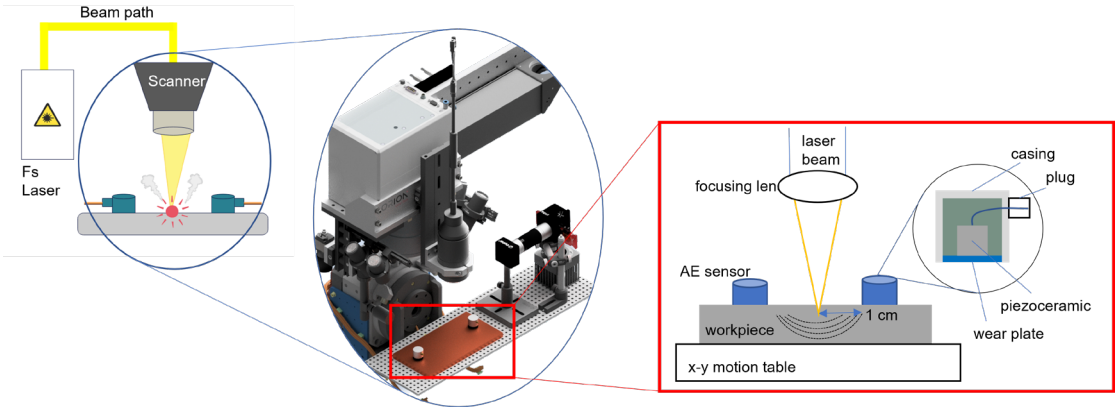

Fig. 2. Schematical illustration of AE process monitoring setup in the fs laser machine

All experimental parts were carried out by irradiating single and multiple fs laser pulses. Each cavity was structured with different laser pulse energies and number of pulses. To investigate the effect of increasing laser pulse energy on the ablation regime and accordingly the AE signal characteristics pulse energy ranging from 10 µJ to 100 µJ were tested. The number of pulses ranging from single and multiple pulses (5, 100) were analyzed. The laser pulse repetition rate was set constant and equal to 200 kHz for all the experimental conditions. Other parameters such as pulse repetition rate, pulse duration and jump speed between pulses were held constant. After laser micromachining, the surface morphology of the ablation crater was characterized with a scanning electron microscope. Samples used for the experiment were non-polished plates of 316L stainless steel with thickness of 1 mm. The single and multi-pulse irradiation of spots were executed in 5 different locations with the distance between the dots is kept at 4 mm (Fig. 3.).

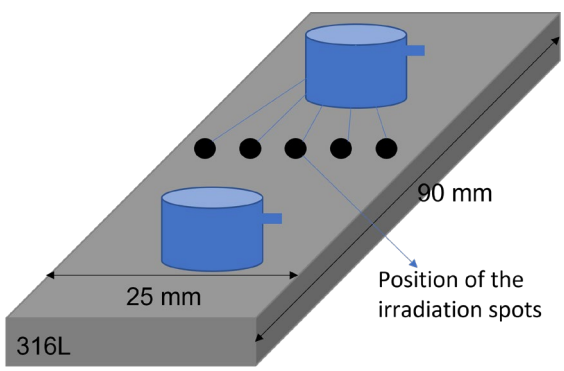

Fig. 3. Schematical illustration of the irradiated spot positions between the AE sensors for single and multi-pulse fs laser ablation experiments

Time domain and frequency domain characteristics analyses are the most commonly-used methods in AE signal processing. Fast Fourier transform (FFT) is a common means of characterization in the frequency domain. Short-time Fourier transform (STFT) and continuous wavelet transform (CWT) can observe the time domain and frequency domain information simultaneously (Xie, Zhang, et al., 2021). In this analysis, RMS of the raw and denoised AE signal is used to characterize the laser irradiating process. Moreover, this paper

focuses mainly on CWT for time-frequency analysis. The CWT is computed using a chosen wavelet function, i.e. Morse wavelet, where the AE signal was convolved with the wavelet at multiple scales. This process results to in a time-frequency representation that effectively captures the temporal and spectral characteristics of the acoustic AE signal. From investigations of time-frequency analysis, a frequency peak at 400kHz is observed to be related to the laser pulses. Therefore, the RMS is also calculated after applying a band pass filter between 380 and 420 kHz which also shows a typical AE event signatures.

3. Results and discussion

The first group of experiments aims to study the relationship between the material removal of 316L ablated by fs laser and the characteristics of AE signals. In the laser irradiating experiments, laser pulse energies of 10, 50 and 100 µJ and a pulse repetition rate of 200 kHz were used to irradiate the 316L substrate at a fixed position with 5 repeated pulses. Fig. 4(a1-a3) shows that circular dots of different sizes are generated by laser ablation, with an increase of diameter of the ablated region as the laser pulse energy increases. Three groups of acoustic emission signals are selected to apply Fast Fourier transform in order to distinguish the signal region from the noise level

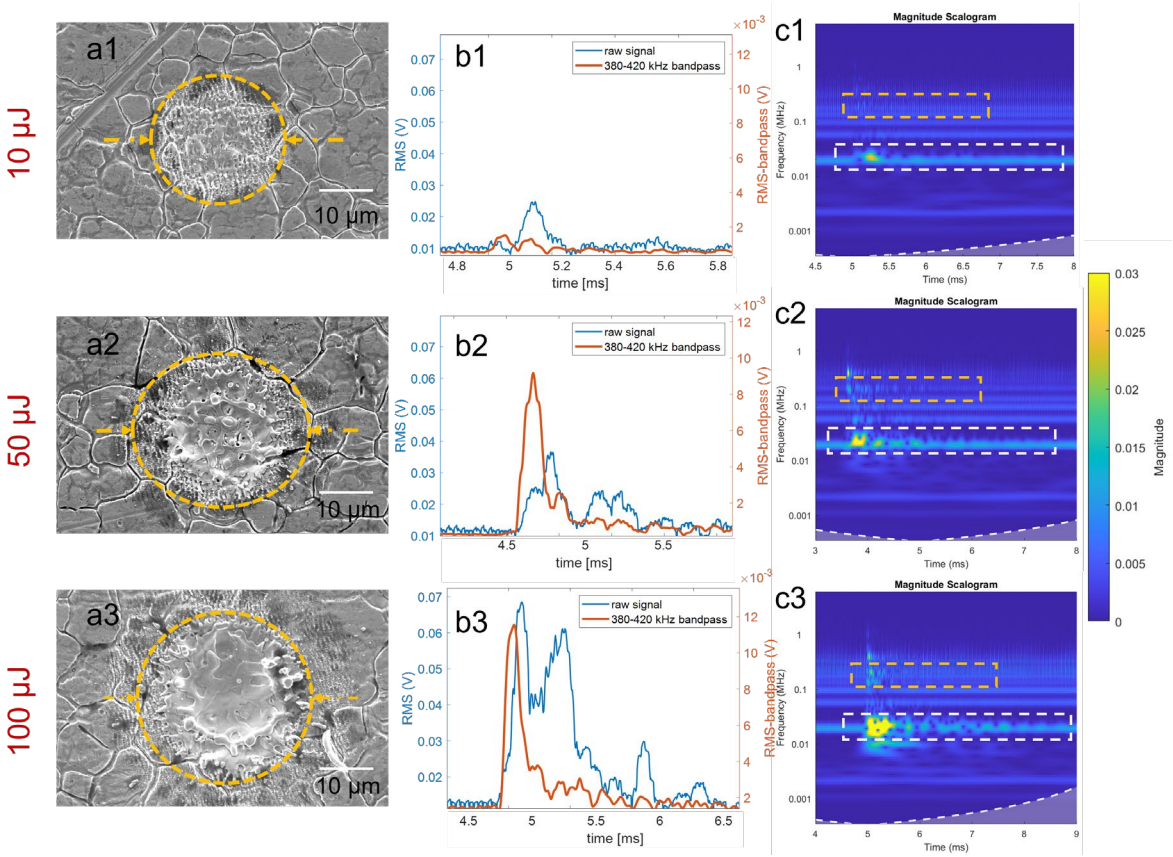

Fig. 4. The change of surface morphology after laser ablation at a laser pulse energy of (a1) 10 µJ, (a2) 50 µJ, and (a3) 100 µJ and each with 5 pulses; (b1), (b2), (b3) RMS curves of corresponding pulse energies of raw and band passed signal; (c1), (c2), (c3) CWT of different pulse energies

When the pulse energy is 10 µJ, a shallow and narrow spot with a diameter of 20.83 ±0.01 µm has been created on the stainless steel. The 316L surface just starts to be ablated in the center of the spot and the material is removed to form a plasma plume. The influence of the removed resolidified material is minimal because the deposited spheres leave no trace on the surface. As pulse energy increases to 50 µJ, the 316L ablated structures seem deeper and become wider (diameter 25.3 ± 0.194 µm). The larger amount of central area material is vaporized, and small spheres of larger diameter are resolidified on the central area, while the edge position morphology shows that the shape of the spheres is similar to the morphology with irradiation of 10 µJ pulse energy. At the pulse energy of 100 µJ, the dot width can be seen to increase further to a diameter of 28.30 ± 0.813 µm. Compared to the irradiated areas with 10 and 50 µJ, the ablation traces are more obvious, and the ablation boundary can be seen clearly. At the same time, the ablated edge forms an area covered by spherical particles whose diameter gradually decreases from the center to the outside.

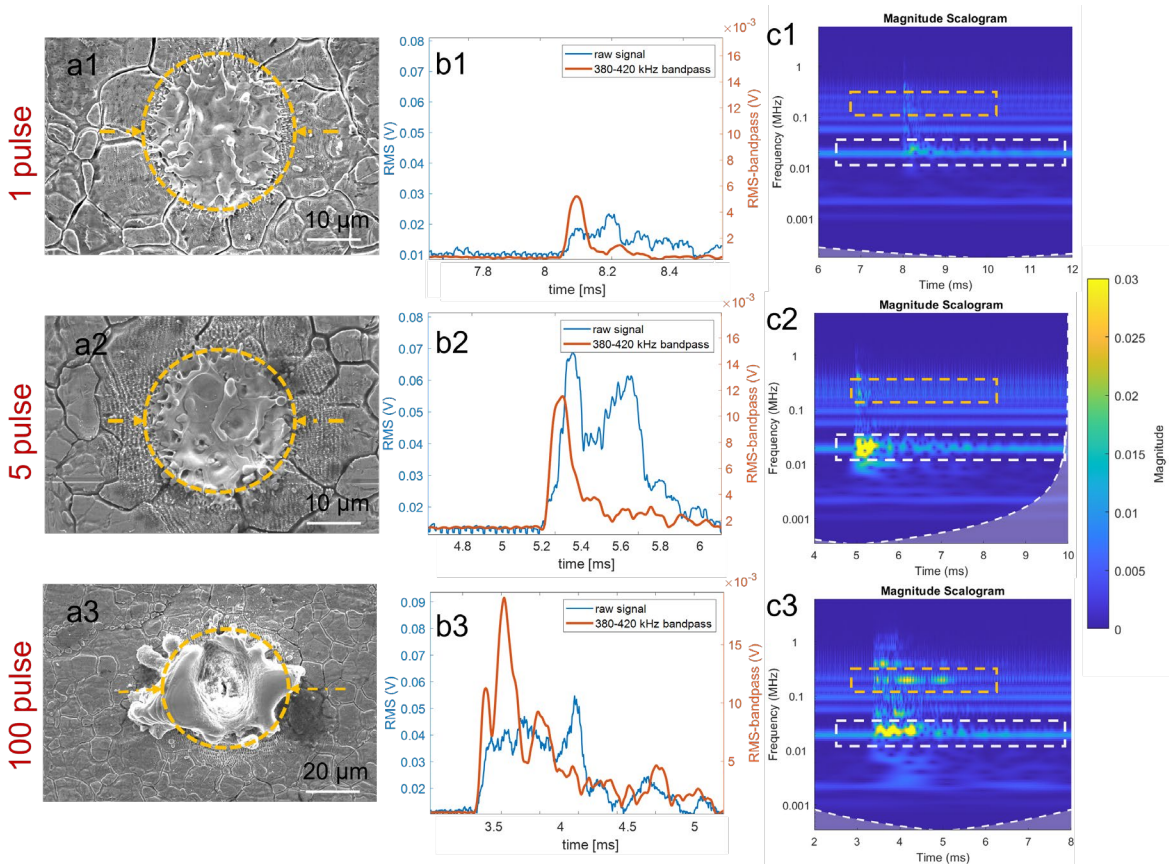

Fig. 5. The change of surface morphology with different number of pulses (a1) 1, (a2) 5, and (a3) 100 at 100 µJ pulse energy; (b1), (b2), (b3) RMS curves of raw and band passed signal ; (c1), (c2), (c3) CWT, for the corresponding number of pulses

The corresponding change in the AE signal can be seen in Fig. 4(b1-b3). When the energy is 10 µJ, both RMS-raw-mean and RMS-bandpass-mean are maintained at low level, 0.0044 V and 0.2311 x 10^{-3} V respectively. With the increase of pulse energy to 50 µJ, the RMS-raw-mean increased to the values around 0.0081 V and RMS-bandpass-mean is increased to 0.0013 V. When the pulse energy reaches 100 µJ, the RMS-

raw-mean and RMS-bandpass-mean increase to 0.0121 V and 0.0017 V, respectively. From the results of frequency domain analysis (Fig. 4(c1-c3).), it can noticed that the frequency bands are mainly distributed in combination with low frequencies between 10 kHz to 100 kHz, fundamental frequency (200 kHz), and multiplies of the fundamental frequency (harmonics of the pulse repetition rate of the fs laser). As expected, it is observed that the magnitude of the CWT signal, i.e. acoustic energy, is positively correlated to the laser pulse energy. The highest magnitudes located in two specific regions as shown in the highlighted regions (white and orange designated frequency bands) in Fig. 4 (c1-c3).

In a second set of experiments, the correlation between the ablation regime and AE signal produced by laser irradiating at several number of pulses (1, 5 and 100) was investigated at the pulse energy of 100 µJ. When the pulse number increases from single pulse to 100 pulses, ablation of the stainless steel occurs at the single pulse (as seen in Fig. 5a1) as the ablation rate increases along with the number of pulses (Fig. 5a2 and 5a3). The depth of ablated crater seems to increase with the number of pulses; however, the excessive energy causes the melting of the material and this material resolidifies around the ablated region. The AE signals are evaluated from the time domain perspective by RMS-raw-mean and RMS-bandpass-mean in Fig. 5(b1-b3). When the pulse number is 1, RMS-raw and RMS-bandpass are 0.0041 V and 0.5592 x 10^{-3} V, respectively. By increasing pulse number to 5, the value of RMS-raw-mean and RMS-bandpass-mean increases to 0.0121 V and 0.0017 V, correspondingly. At 100 pulses, the number of peaks of the AE signal waveform increases significantly and shifts the RMS-raw-mean and RMS-bandpass-mean amplitude range to 0.0127 V and 0.0035 V with an increase in the range of fluctuation. Fig. 5 (c1-c3) displays the frequency domain analysis of the AE signal, where an increase in the number of pulses results in a brighter lower frequency region (10 kHz to 100 kHz) with gradually increasing intensity. The dominant frequency of different pulse numbers is located around the 200 kHz pulse repetition range and its harmonics, with the strongest frequency being 400 kHz. This finding is consistent with previous results on increasing number of pulses. The highest magnitudes located in two specific regions as shown in the highlighted regions (white and orange designated frequency bands). Also, the effect of melting and resolidification based on excessive energy can be seen from the specific magnitude in Fig. 5 (c3), orange box. Further study is needed to validate the effect of melting and solidification on the AE signal waveform trend.

From the results, it is obvious that the increase in pulse energy and the number of pulses leads to an increase in the energy absorbed by the material, which is thermally vaporized to produce a larger ablation region. As the material ablation increases due to the number of pulses or pulse energy, the number of AE events increases, resulting an increase in signal intensity. This increase in signal intensity means that the AE events are added constructively, probably because of the very high pulse repetition rate. Therefore, it can be assumed that the ablation quality in terms of resultant surface morphology has a positive correlation with the AE signal at different laser pulse energies. Moreover, it can be seen from the band-passed signal that the adequate bandpass filter allows to subtract the process relative AE waveform. The increase in pulse energy was from 10 µJ to 50 µJ and 100 µJ. The RMS values exhibited a percentage increase of 84.1% from 0.0044 to 0.0081 and 49.4% from 0.0081 to 0.0121. Thus, a correlation was observed between the increase in pulse energy and the corresponding percentage increase in RMS values. In the second experimentation, the increase in the number of pulses was from 1 pulse to 5 pulses and 100 pulses. Correspondingly, the RMS values exhibited a percentage increase of 195.1% from 0.0041 to 0.0121, followed by a slight increase of 5% from 0.0121 to 0.0127. Importantly, it was observed that further increasing the number of pulses beyond 5 did not yield a significant change in the RMS values. The results of these experiments provided valuable insights into the relationship between the AE signals and the ablation process, which can be used to optimize the process for various applications.

4. Conclusion

In this manuscript, the effect of AE technique to evaluate the fs ablation on 316L stainless steel was studied. By combining the characteristics of the AE signal with the ablation quality of fs laser machining, the feasibility of using AE technology to monitor the fs laser machining was analyzed. Single- and multi-pulse fs laser dotting experiments were carried out. The main findings in the pulsed laser experiments under the processing conditions and analyzed material were as follows: (1) The ablation diameter has a positive correlation with the AE signal at different laser pulse energies and number of pulses. (2) The combined AE characteristic trends such as RMS, and signal range could be used as an indicator to classify the processing regime and the resultant ablated surface morphology/quality by distinguishing the ablation regime as sufficient ablation or melting. (3) There was a significant improvement in the accuracy of the AE signal analysis after applying a bandpass filter, which allowed for better identification and classification of the different ablation modes.

Acknowledgement

This work was partially funded by the KU Leuven C3 IOF project fs-SPR (C3/20/084) and the Research Foundation - Flanders (FWO-Vlaanderen) Medium-Scale Research Infrastructure project FemtoFac (I001120N).

References

Bornschlegel, B., & 2020 In-situ analysis of heat accumulation during ultrashort pulsed laser ablation. J. Laser Micro Nanoeng.

Bhuiyan, M., Choudhury, I., Dahari, M., & 2016. Application of acoustic emission sensor to investigate the frequency of tool wear and plastic deformation in tool condition monitoring. Elsevier.

Bordatchev, E., & 2006. Effect of focus position on informational properties of acoustic emission generated by laser–material interactions. Elsevier.

Chethan, Y., Ravindra, H., & 2019. Optimization of machining parameters in turning Nimonic-75 using machine vision and acoustic emission signals by Taguchi technique. Elsevier.

Francois, M., Sun, A., King, W., & 2017. Modeling of additive manufacturing processes for metals: Challenges and opportunities. Elsevier.

Hamad, A., & 2016. Effects of different laser pulse regimes (nanosecond, picosecond and femtosecond) on the ablation of materials for production of nanoparticles in liquid.

Ion, J., &2005. Laser processing of engineering materials: principles, procedure and industrial application.

Kacaras, A., Bächle, M., Schwabe, M., Zanger, F., & 2019. Acoustic emission-based characterization of focal position during ultra-short pulse laser ablation. Elsevier.

Kek, T., & 2009. AE signals as laser cutting quality indicators.

Le Harzic, R., Sommer, S., Le Harzic, R., Breitling, D., Weikert, M., Sommer, S., Föhl, C., Valette, S., Donnet, C., Audouard, E., & Dausinger, F., & 2005 Pulse width and energy influence on laser micromachining of metals in a range of 100 fs to 5 ps. Elsevier.

Lee, D. E., Hwang, I., Valente, C. M. O., Oliveira, J. F. G., & Dornfeld, D. A., & 2006. Precision Manufacturing Process Monitoring with Acoustic Emission. Condition Monitoring and Control for Intelligent Manufacturing.

Li, X., Guan, Y., & 2020. Theoretical fundamentals of short pulse laser-metal interaction: A review. Nanotechnology and Precision Engineering.

Linde, D. Von der, & 2000. The physical mechanisms of short-pulse laser ablation. Elsevier.

Lu, M.-C., Chiou, S.-J., Kuo, B.-S., Chen, M.-Z., Rodríguez-Martín, M., & Rodríguez-Gonzálvez, P., & 2021. Analysis of Acoustic Emission (AE) Signals for Quality Monitoring of Laser Lap Microwelding.

Liu, G., Chen, S., Li, Z., Liu, L., & 2018. Review of optical coherence tomography in micro/nanomanufacturing. IEEE Journal of Selected Topics in Quantum Electronics.

Mazur, E., Phillips, K. C., Gandhi, H. H., & Sundaram, S. K., & 2015. Ultrafast laser processing of materials: a review. Advances in Optics and Photonics.

Mozaffar, M., Liao, S., Xie, X., Saha, S., Park, C., Cao, J., Liu, W. K., & Gan, Z. Mechanistic artificial intelligence (mechanistic-AI) for modeling, design, and control of advanced manufacturing processes: Current state and perspectives. Elsevier.

Nemeth, A., & 2013. Optical coherence tomography–applications in non-destructive testing and evaluation.

Orazi, L., Romoli, L., Schmidt, M., Annals, & 2021. Ultrafast laser manufacturing: from physics to industrial applications. Elsevier.

Ostendorf, A., Korte, F., Kamlage, G., Klug, U., Koch, J., Serbin, J., Baersch, N., Bauer, T., Chichkov, B. N. & 2006. Applications of Femtosecond Lasers in 3D Machining. 3D Laser Microfabrication.

Roozbahani, H., Salminen, A., Manninen, M., & 2017. Real-time online monitoring of nanosecond pulsed laser scribing process utilizing spectrometer. J. Laser Appl.

Rußbüldt, P., Mans, T., & 2010. Powerscaling of Ultrafast Lasers: New Solid State Lasers Pave the Way to Transfer Femtosecond Technology to Industry. Wiley Online Library.

Schmitt, R., & 2013. Process monitoring in laser micro machining.

Singha, S., Hu, Z., & Gordon, R. J., & 2008. Ablation and plasma emission produced by dual femtosecond laser pulses. *Journal of Applied Physics*.

Terchi, A., Au, Y. H. J. & 2001. Acoustic emission signal processing. Measurement and Control.

Xie, X., Huang, Q., Long, J., Ren, Q., Hu, W., & 2020. A new monitoring method for metal rust removal states in pulsed laser derusting via acoustic emission techniques. Elsevier.

Xie, X., Zhang, Y., Huang, Q., Huang, Y., & 2021. Monitoring method for femtosecond laser modification of silicon carbide via acoustic emission techniques. Elsevier.

Wiesemann, W., & 2004. 2.8 Process monitoring and closed-loop control. Springer.

Yang, R., Huang, Y., Rong, Y., Wu, C., & 2022. Evaluation and classification of CFRP kerf width by acoustic emission in nanosecond laser cutting. Elsevier.